

# Novel DC to Single-Phase Isolated AC Converter using Coupled Inductor with Power Decoupling Capability

Nagisa Takaoka, Keisuke Kusaka, Hayato Higa, Jun-ichi Itoh  
Nagaoka University of Technology  
1603-1 Kamitomioka-machi  
Nagaoka city Niigata, Japan  
Tel., Fax: +81 / (258) – 47.9533.

E-Mail: ntakaoka@stn.nagaokaut.ac.jp, kusaka@vos.nagaokaut.ac.jp,  
hhiga@stn.nagaokaut.ac.jp, itoh@vos.nagaokaut.ac.jp  
URL: <http://itohserver01.nagaokaut.ac.jp/itohlab/index.html>

## Keywords

«Converter circuit», «Power converters for EV», «Power conditioning», «Single phase system»

## Abstract

This paper proposes a novel active power decoupling converter topology, where additional components are not necessary in order to minimize the power decoupling circuit. In conventional EV/PHV battery charger systems with the power decoupling capability require several passive components and switching devices in order to absorb the power ripple at twice grid frequency. Thus, these topologies restrict the downsizing. In order to avoid the additional components for the power decoupling capability, this paper proposes the isolated DC to single-phase AC converter with an employment of a coupled inductor. This converter consists of a full-bridge inverter, a high frequency transformer and an indirect matrix converter in order to eliminate DC-link smoothing capacitors. Moreover, the additional inductor for the power decoupling circuit in the conventional topology can be substituted with leakage inductor of the coupled inductor in the proposed converter. In the proposed circuit, the coupled inductor is an isolation between the DC and the AC equipment for safety and the boost inductance. These characteristics result in a high-power-density converter. The validity of the proposed circuit is experimentally confirmed by a simulation and experiment at prototype. As a simulation result, the proposed method reduces the second-order harmonic of the power ripple by 97.5% at 3-kW of the output power. As experimental results, the proposed converter reduces the DC current ripple generated by a single-phase AC load by 46.5%.

## I. Introduction

Recently, due to an increasing focus on energy saving, research on PHV/EV has been rapidly expanded [1-3]. As a main component of a battery charger for these vehicles, a DC to single-phase AC isolated converter is employed in order to provide a safe connection between DC bus and general single-phase AC equipment. Downsizing and long life-time are required for the DC to single-phase AC isolated converters. In this converter, DC bus voltage has a power ripple at twice the grid frequency which is caused by instantaneous power mismatch between the DC side and the single-phase AC grid side. A large capacitance value of the DC-link capacitor is required in the DC-link to absorb the power ripple in the conventional method, leading to the use of bulky electrolytic capacitors. However, these bulky electrolytic capacitors limit life-time and the downsizing of the DC to single-phase AC converters.

In order to solve these problems, many circuit topologies with the power decoupling capability have been studied [4-11]. In particular, these circuit topologies employ passive components and several additional switching devices for power decoupling capability, which is defined as active power decoupling capability. In such active power decoupling capability, the capacitor voltage is actively fluctuated, so only small capacitance value is required and replaced with a film capacitor or ceramic

capacitor. Thus, these systems with the active power decoupling capability achieve the long life-time because the bulky electrolytic capacitors are eliminated. Focusing on [4], the DC to single-phase AC non-isolated converter is introduced as a simple configuration with the power decoupling circuit constructed in the third leg of the full bridge inverter. This topology controls the buffer capacitor voltage of the power decoupling circuit using two additional switching devices and an additional inductor. This additional inductor prevents the minimization of the converter.

In order to avoid the additional magnetic component, the DC to single-phase isolated converters with boost-type topologies are also studied. These converters consist of a fly-back-type inverter and additional switching devices for the buffer circuit. Although the employment of the fly-back-type topology eliminates the additional inductor, the power capacity of the fly-back-type topology is limited in term of the converter-efficiency. As a conclusion, the conventional topologies in [4-9] require either the additional switching devices or the additional inductor for the power decoupling circuit. This leads to a low efficiency and difficulties in downsizing.

This paper proposes a novel DC to single-phase AC isolated converter using the coupled inductor to achieve the power decoupling capability. A boost converter with coupled inductor is applied in the proposed circuit because this topology reduces both inductor volume and conduction loss compared to conventional boost topologies [12-13]. Therefore, an interleaved topology of the boost converters with coupled inductor is suitable to employ as a primary-side converter of the DC to single-phase AC isolated converter.

The originality of this paper is that the transformer between the DC side and the AC side is integrated as the coupled inductor in order to eliminate any additional switching devices or any additional inductor for the power decoupling capability. In particular, the primary-side converter of the proposed system is comprised of a full bridge inverter, which also operates as two-phase interleaved boost converters to boost the voltage of small capacitors, which absorb the power ripple. Owing to the boost converters, the buffer capacitor voltage can be pushed up higher than the DC input voltage. Consequently, the buffer capacitance for the power decoupling circuit is reduced by the fluctuation of the buffer capacitor at high voltage. Moreover, the additional inductor for the power decoupling circuit in the conventional topology is substituted with a leakage inductor of the coupled inductor in the proposed converter; meanwhile, the additional switching devices are unnecessary because the primary-side converters are operated as a power decoupling circuit during the common-mode of the coupled inductor. On the other hand, the secondary-side converter can reduce the switching loss because the secondary-side converter is operated at the twice grid frequency. Thus, the proposed converter achieve the downsizing and the long-lifetime by the elimination of the additional components.

This paper is organized as follows; first, the proposed converter for the DC to single-phase AC converter and the principle of the power decoupling method are introduced; second, the operation mode of the proposed converter and the modulation methods with power decoupling capability are explained; finally, the fundamental operation waveforms of the proposed converter are evaluated in simulations and experiments.

## II. Circuit Topology

### A. *Conventional Circuit*

Figure 1 depicts a conventional isolated converter for the DC to single-phase AC converter. The conventional topology consists of an interleaved boost converter, an isolated DC to DC converter and an H-bridge inverter. The interleaved boost converter at the primary-side in the conventional system is required in order to push the low input voltage, e.g. the low voltage of the photovoltaic panel, up to the voltage higher than the peak voltage of the single-phase grid voltage. This two-phase interleaved topology is employed to reduce the conduction loss and the volume of the boost inductor by dividing the current by half. In addition, the full-bridge inverter at the primary side of the isolated DC to DC converter generates a high-frequency square voltage, which can reduce the volume of the transformer. In this topology, the DC current has a power ripple component caused by the single-phase AC side. Thus, a bulky electrolytic capacitor  $C_{dc2}$  is required in the DC-link in order to compensate the power ripple. However, this capacitor  $C_{dc2}$  limits the converter's life-time.

Figure 2 depicts a conventional isolated DC-single-phase-AC converter with the conventional power decoupling circuit. This power decoupling circuit is applied at the output of the boost circuit in order to eliminate the bulky electrolytic capacitor. In the conventional power decoupling method, the buffer capacitor voltage is actively fluctuated in order to absorb the power ripple. Therefore, the DC-link capacitor value can be minimized in comparison with that in Fig. 1 because the power ripple is compensated by the high voltage fluctuation at the small buffer capacitance of  $C_{buf}$ . However, the conventional power decoupling method requires additional switching devices and magnetic components. Consequently, this method increases the volume of the cooling system and the converter loss.

### B. Proposed Circuit

Figure 3 presents the proposed isolated DC to single-phase AC converter. The proposed converter consists of an indirect matrix converter and an interleaved boost converter with the coupled inductor. The third winding of the coupled inductor is electrically isolated to the primary side in order to transfer the power to the secondary side. A buffer capacitor  $C_{buf}$  and a boost inductor  $L_{boost}$  contributes to the power ripple compensation. In particular, the charge and the discharge of  $C_{buf}$  compensate the power ripple, whereas the boost-inductor current  $i_{bc}$  is controlled by the interleaved boost converter. Furthermore, in the proposed converter, the applying the three-winding inductor achieves the DC current control and the grid current control at the same time. In particular, the DC current control is employed with a common-mode operation of the three-winding inductor, whereas the grid current control is implemented with a differential-mode operation. Consequently, the system with the power decoupling capability operates the two current controls without additional switching devices and buffer inductors owing to the employment of the three-winding coupled inductor.

The indirect matrix converter in the secondary side is employed to eliminate the DC-link smoothing capacitors in a conventional Back-to-Back system. The indirect matrix converter performs the rectifier operation and the polarity reversion of the input voltage to output the grid voltage. Therefore, the DC/AC conversion of the indirect matrix converter is achieved with the significant loss reduction of the switching loss because the switching is operated at twice the grid frequency. It is should be noted that

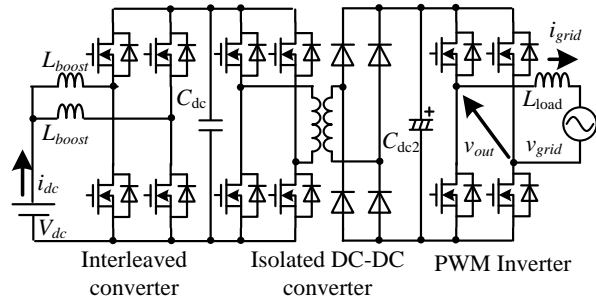


Figure 1. Conventional isolated DC to single-phase AC converter with interleaved boost topology. The conventional converter uses a bulky electrolytic capacitor  $C_{dc}$  to absorb the power ripple caused by a single-phase load.

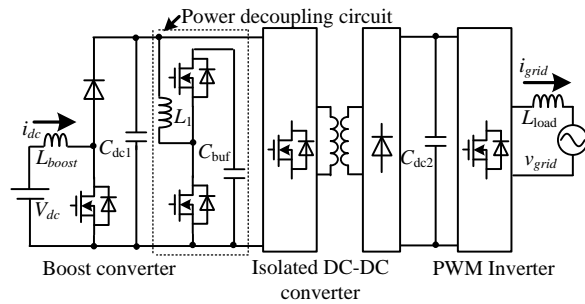


Figure 2. Conventional isolated DC to single-phase AC converter with active buffer circuit. The conventional converter uses a bulky electrolytic capacitor  $C_{dc}$  to absorb the power ripple caused by a single-phase load.

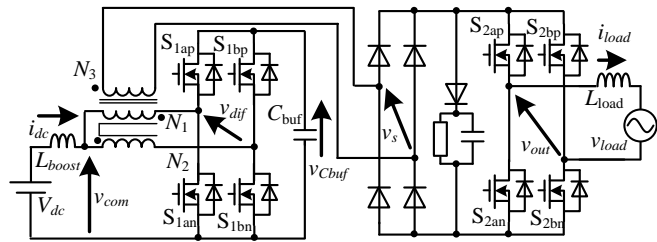


Figure 3. Proposed isolated DC to single-phase AC converter. The primary-side converter together with the coupled inductor and the buffer capacitor are controlled in order to convert the DC input power to the AC power and absorb the power ripple without additional switching devices and inductors.

in case of the required bi-directional operation, a full bridge inverter is applied instead the diode rectifier of the indirect matrix converter.

### III. Control Strategy

#### A. Principal of power decoupling

Figure 4 depicts the principle of the power decoupling method in this section. This power decoupling method is achieved by the compensation of the power ripple in the DC-link voltage with a small capacitance  $C_{buf}$ . If the grid current  $i_{grid}$  is sinusoidal waveform and the unity power factor is achieved, an instantaneous output power  $p_{out}$  is expressed by the following:

$$\begin{aligned} p_{out} &= \sqrt{2}V_{load} \sin(\omega_o t) \cdot \sqrt{2}I_{load} \sin(\omega_o t) \\ &= V_{load} I_{load} \{1 - \cos(2\omega_o t)\} \\ &= P_{ave} - P_{ave} \cos(2\omega_o t) \end{aligned} \quad (1)$$

where  $V_{load}$  is the root-mean-square values of the output voltage,  $I_{load}$  is the RMS value of the output current,  $P_{ave}$  is the average output power and  $\omega_o$  is the grid-side angular frequency. The ripple component shown as the second term on the right side of (1) should be eliminated in order to obtain a constant DC current in the DC side. Note that other topologies which absorb the power ripple, for example C-L-C topology, are not effective to reduce the volume of the conventional circuit.

$$p_{buf} = P_{ave} \cos(2\omega_o t) \quad (2)$$

The polarity of the buffer power is defined to be positive when the buffer capacitor is charged. The buffer capacitor voltage  $v_{Cbuf}$  which needs to absorb the power ripple is calculated based on the energy of the buffer capacitor. First, the energy of the buffer capacitor  $W_{Cbuf}$  is expressed by a voltage-current equation of a capacitor and (2).

$$\begin{aligned} W_{Cbuf} &= \int_{t_0}^t v_{Cbuf} \left( C_{buf} \frac{dv_{Cbuf}}{d\tau} \right) d\tau \\ &= \int_{t_0}^t P_{ave} \cos(2\omega_o \tau) d\tau \end{aligned} \quad (3)$$

where  $t_0$  is a start time of operation. By using (3), the buffer capacitor voltage to compensate the power ripple is presented by the following:

$$v_{Cbuf} = \sqrt{V_{C0}^2 + \frac{P_{ave}}{\omega_o C_{buf}} \{ \sin(2\omega_o t) - \sin(2\omega_o t_0) \}} \quad (4)$$

where  $V_{C0}$  is the buffer capacitor voltage at a start time. If  $t_0$  is zero, (4) is rewritten as (5).

$$v_{Cbuf} = \sqrt{V_{C0}^2 + \frac{P_{ave}}{\omega_o C_{buf}} \sin(2\omega_o t)} \quad (5)$$

In the proposed circuit, the DC current flowing to the coupled inductor from DC supply is controlled as a constant DC value. Thus, the buffer capacitor voltage has the power ripple components. The proposed converter with the power decoupling capability is achieved, whose result is that the power ripple component at DC side is absorbed.

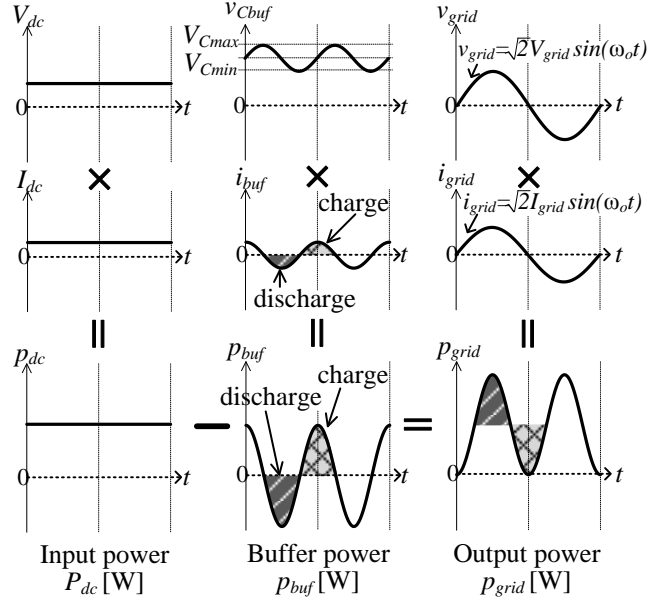


Fig. 4. Relationship among each waveforms.

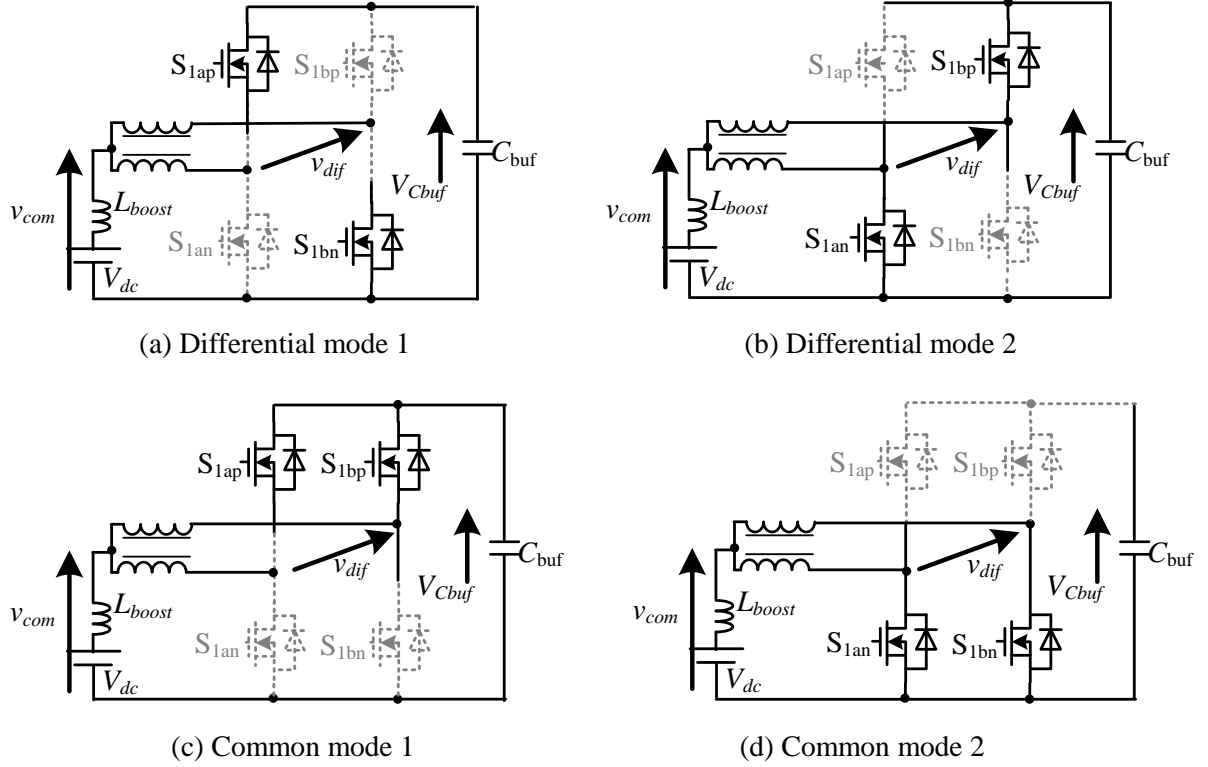


Fig. 5. Operation modes of primary-side converter with coupled inductor. The primary side of the proposed system is operated in two modes; the differential mode when the power is delivered to the secondary-side and the common mode when the power ripple is adsorbed.

### B. Duty calculation

Figure 5 depicts the operation modes of the primary-side converter with the coupled inductor. The proposed primary-side converter has four operation modes which generate a phase difference between the switching of each arm as an interleaved converter. The boost inductor  $L_{boost}$  is considered as a leakage inductor of the coupled inductor. Therefore, if the inductance value of the leakage inductor is insufficient for the design value, a small inductor is added. In the proposed system, the differential-mode voltage of the coupled inductor is controlled to generate the output current, whereas the common-mode voltage is controlled to perform the power decoupling capability. In the control of the differential-mode voltage, the three-winding voltage of the coupled inductor is controlled into a three-level voltage by operation modes as shown in Fig. 5 (a) and (b). On the other hand, the common-mode voltage  $v_{com}$  is controlled to absorb the power ripple in the control of the common-mode voltage. In particular, the power ripple component occurs in the buffer capacitor voltage, because the DC current is regulated into a constant value in the proposed power decoupling method. Moreover, the proposed power decoupling capability consists of a boost topology. The coupled inductor is boosted the fluctuation of the buffer capacitor voltage in bigger than the DC voltage  $V_{dc}$ . The capacitance of the buffer capacitor is achieved to reduce enough to increase the fluctuated voltage of the buffer capacitor to absorb the power ripple. Thus, the proposed converter with the boost topology of the power decoupling capability is achieved to reduce the capacitance than a buck-type topology of the one.

In the proposed method, each duties of the primary converter in one carrier period requires to meet a following equation (6).

$$1 = d_{dif\_a} + d_{dif\_b} + d_{com\_c} + d_{com\_d} \quad (6)$$

where  $d_{dif\_a}$  and  $d_{dif\_b}$  are the duties of the differential mode as shown in Fig. 5(a) and (b), whereas  $d_{com\_c}$  and  $d_{com\_d}$  are the duties of the common mode as shown in Fig. 5(c) and (d). If the output voltage is controlled into a sinusoidal waveform, the voltage pulses between the first and second winding are controlled as PWM pulses. The sum of the differential-mode duties  $d_{dif}$  is expressed as follows:

$$d_{dif} = d_{dif\_a} + d_{dif\_b} = \frac{v_{out}^*}{2V_{dc}} = \frac{\sqrt{2}V_{load} \sin(\omega t)}{2V_{dc}} \quad (7)$$

where  $v_{out}^*$  is a reference of the output voltage.

Then, the common mode of the proposed method is applied the remaining period after the differential mode. Therefore, the duty of the common mode is calculated by the following:

$$d_{com\_c} = (1 - d_{dif}) \frac{v_{com}^*}{2V_{dc}} \quad (8)$$

where  $v_{com}^*$  is a reference of the common voltage and is output by a PI control of the DC current as explained in the next section.

Figure 6 depicts a relationship among each reference, the triangle carrier and the switching pattern of the primary converter in the proposed system. In the differential voltage mode, the differential voltage pulses between the first and second winding are controlled as PWM pulses. Then, the voltage the period of the each duties as shown in Fig. 5(a) and (b) in a carrier period is needed to be equal in order to suppress a DC biased magnetization of the coupled inductor, especially. The comprising signals A and B is generated by comprised duties which the sum of  $d_{com\_c}$  and  $d_{dif}$  and only  $d_{com\_c}$  and a triangle carrier as shown in Fig. 6. Thus, the desired operation in each duties of the primary converter is actualized as described previously. The primary converter of the proposed system achieves the power decoupling operation and the transfer power to the secondary side as a same time without the additional passive components and the switching devices.

### C. Control Strategy

Figure 7 shows the control block diagram of the proposed system with the power decoupling capability. The current controls and voltage controls are employed with PI controllers. The DC current is controlled to a constant DC value to absorb the power ripple component. This DC current control is applying as a minor loop of the buffer capacitor voltage control. This buffer capacitor control controls only the average of the buffer capacitor voltage  $v_{Cbuf\_ave}$  in order to avoid the divergence of  $v_{Cbuf\_ave}$ . The average value of the buffer capacitor voltage  $v_{Cbuf\_ave}$  is twice of the

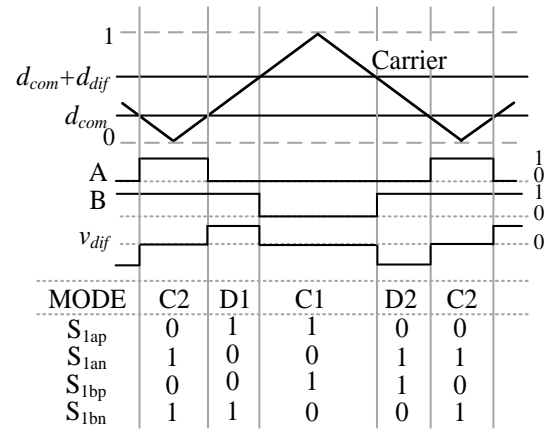


Fig. 6. Current and voltage operating waveforms of proposed converter with power decoupling capability. The buffer capacitor voltage absorbing the ripple component is controlled by the zero-voltage period of the primary-side transformer voltage.

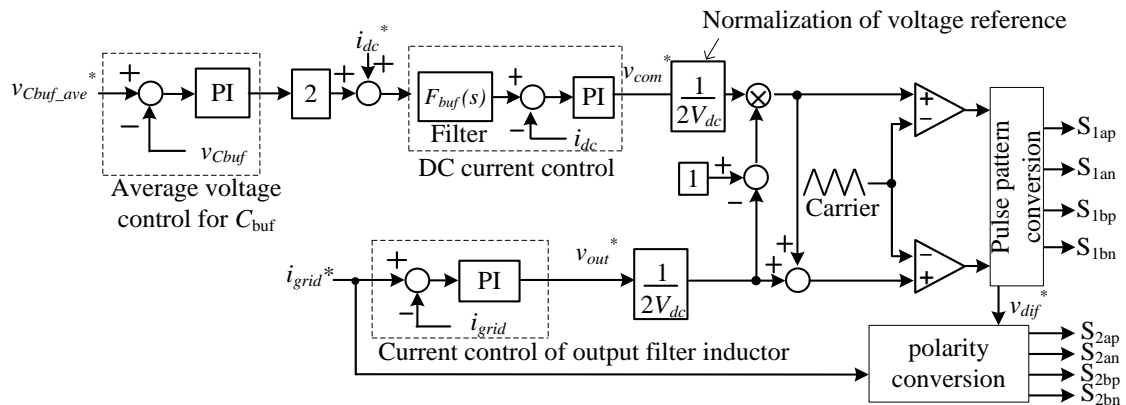


Fig. 7. Proposed control block diagram. The DC current is controlled to absorb power ripple. The buffer capacitor voltage control is employed in order to avoid the divergence of the average voltage due to discretization.

TABLE I  
SYSTEM PARAMETERS.

DC bus voltage	200 V <sub>dc</sub>	Load voltage	200 V <sub>rms</sub>
Rated power	3 kW	Load frequency	50 Hz
Boost L ( $L_{boost}$ )	1.1 mH	Filter L ( $L_{load}$ )	2.0 mH
Buffer C ( $C_{buf}$ )	150 $\mu$ F	Turn ratio of coupled inductor $N_1:N_2:N_3$	1 : 1 : 2
Load current	15 A <sub>rms</sub>		
Carrier frequency of full bridge inverter	50 kHz	Natural angular frequency of buffer C voltage control	30 rad/s
Natural angular frequency of DC current control	6000 rad/s	Natural angular frequency of load current control	4000 rad/s
Damping factor of DC current control	0.7	Damping factor of buffer C voltage control	1.0

common voltage  $v_{com}$ . In the proposed converter, the output current is controlled by the full bridge inverter at the primary side. Then, the diode bridge rectifiers the differential-mode voltage, whereas the full bridge inverter at the secondary side operates a unfold and changes the polarity of the voltage pulse in responding to the polarity of the grid voltage. Thus, the secondary-side converter achieves the reduction of the switching loss.

## IV. Simulation and Experimental Results

### A. Simulation results in steady state

The performances of the proposed circuit are verified by simulation and experiment.

Table I shows the simulation condition for the proposed isolated DC-single-phase-AC-converter with the power decoupling capability. It should be noted that in the confirmation operation without the power decoupling capability, the simulation and experimental results of the power ripple component is acquired under the conditions that the gain of the DC current controller is reduced and the gain of the average voltage controller of the buffer capacitor  $C_{buf}$  is increased.

Figure 8 and Figure 9 show the input and the output waveforms with/without the proposed power decoupling method, respectively. A input current is filtered with a LPF with a cut-off frequency of 1 kHz in order to remove a switching ripple. Fig. 8 shows the result without the power decoupling method. Thus, the input current has a power ripple component at 100 Hz because the power ripple component is not compensated by buffer capacitor in this operation mode. Then, the ripple component is 127.1% with reference to an average current in Fig. 8. In contrast, as shown Fig. 9, the proposed power decoupling

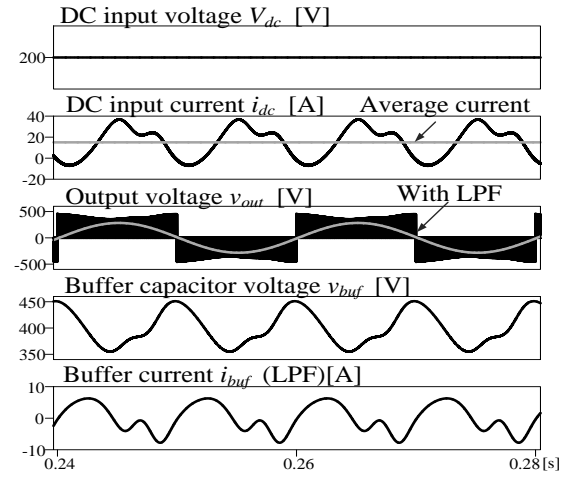


Fig. 8. Waveforms without proposed power decoupling method in steady state.

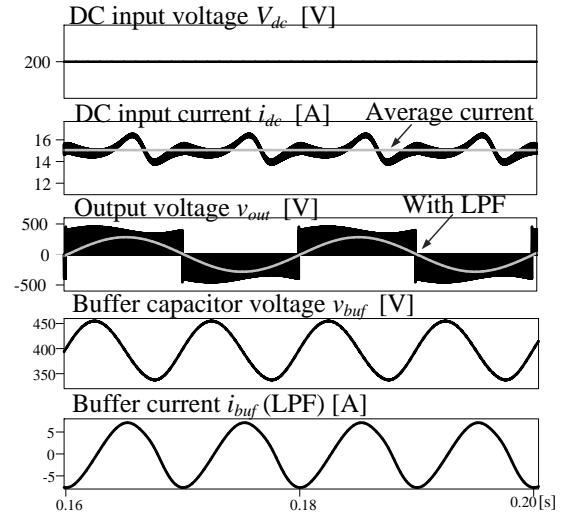


Fig. 9. Waveforms with power decoupling method in steady state. The proposed power decoupling method reduces the power ripple component at 100 Hz on the input current by 97.5%.

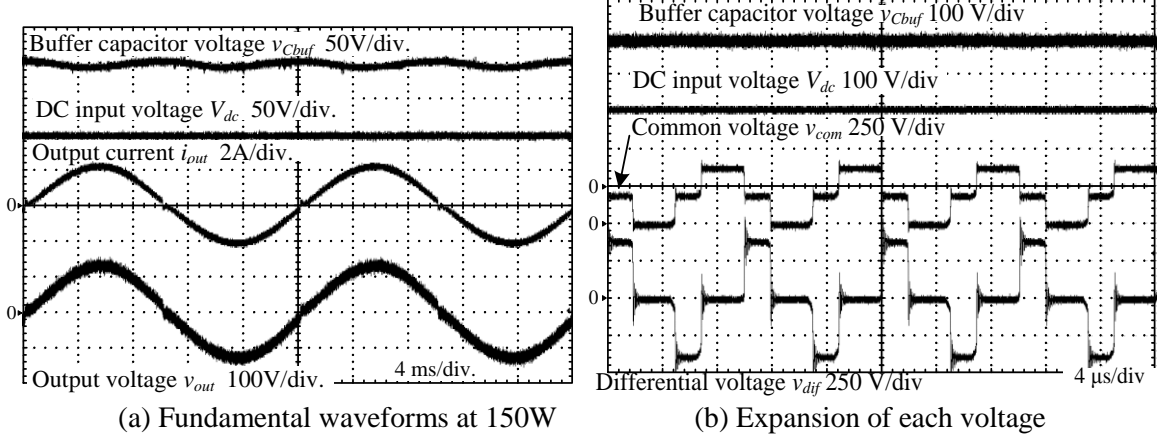


Fig. 10. Waveforms with power decoupling method in steady state. The zero voltage period of  $v_{dif}$  is agreed with the  $V_{dc}$  period of  $v_{com}$ .

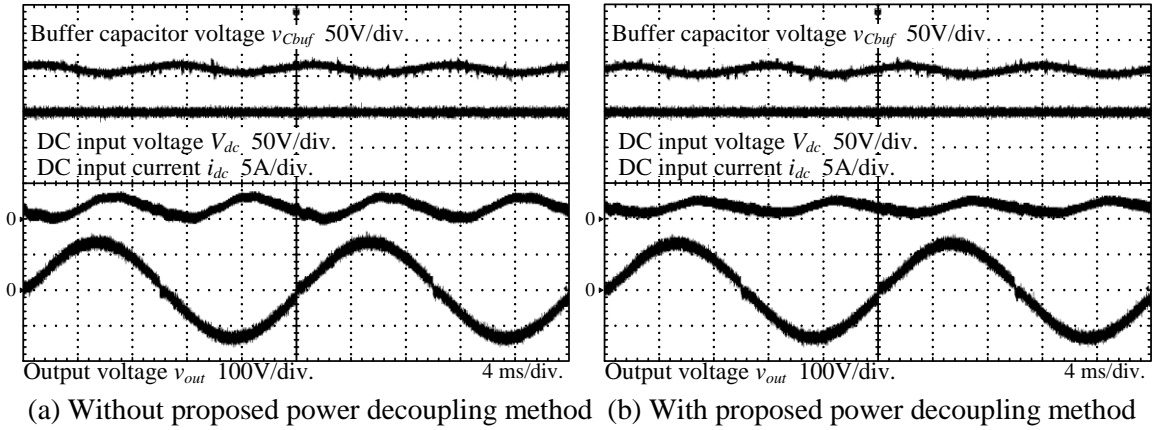


Fig. 11. Experimental waveforms with/without power decoupling method in steady state.

method is controlled to actively fluctuate the buffer capacitor voltage  $v_{cbuf}$ . Consequently, the secondary-order harmonics in the DC input current is suppressed greatly. As a result, the ripple of the DC input current is suppressed by 97.5%.

### B. Experimental results

Figure 10 (a) depicts the experimental waveform of the input and output voltage and Figure 10 (b) depicts the extended waveform of the coupled inductor in the proposed converter with open-loop control of the load current control. It should be noted that these experimental results are obtained with a natural angle frequency of the input current control of 4000 rad/s, a buffer capacitor of 200  $\mu\text{F}$ ,  $v_{out}$  of 100  $\text{V}_{\text{rms}}$  and an R-L load as the single-phase AC load. The boost operation, which pushed the voltage of the buffer capacitor higher than that of the DC voltage  $V_{dc}$ , is confirmed by Fig. 10 (a). On the other hand, as shown Fig.10 (b), the differential-mode voltage  $v_{dif}$  is a three-level voltage waveform, which is combined of  $+v_{Cbuf}$ ,  $-v_{Cbuf}$ , and a zero voltage period. This zero voltage periods of  $v_{dif}$  in the power ripple operation is decided by the capacitance of  $C_{buf}$  and the output power. Moreover, the period of the zero level in the differential voltage is utilized with the top and bottom level of the common mode voltage. Thus, the power decoupling operation and the output current control are achieved at the same time. Through these results, the operation of the primary-side converter with the power decoupling operation in the proposed system is confirmed without additional switching devices and magnetic components.

Figure 11 shows the waveforms of the proposed converter with/without the proposed power decoupling method, respectively with  $V_{dc}$  of 150 V and  $v_{out}$  of 100  $\text{V}_{\text{rms}}$ . As shown in Fig.11 (a), the DC input current has a power ripple component at second-order harmonics of the grid frequency. The buffer

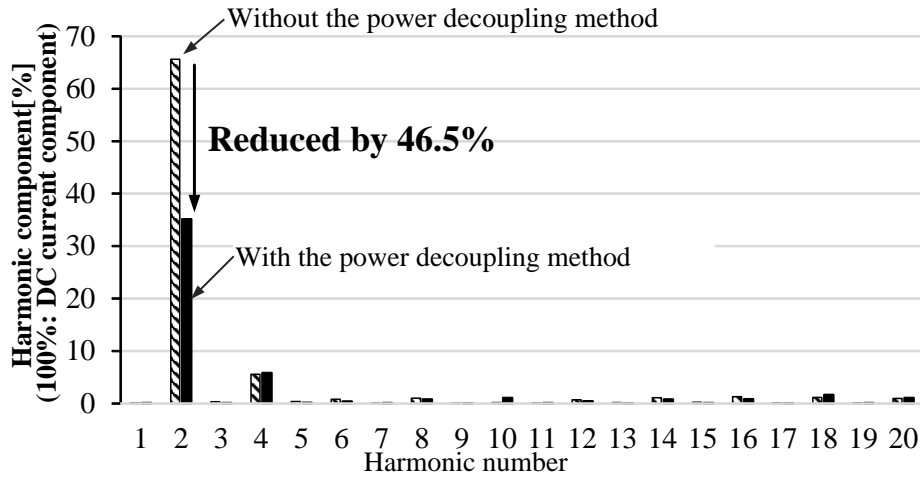


Fig. 12. Harmonic analysis of DC input current.

capacitor voltage fluctuation is small because the power ripple component is not compensated by buffer capacitor in this operation mode, i.e. the passive power decoupling capability. Therefore, the capacitance of the buffer capacitor  $C_{buf}$  is smaller than the necessary capacitance to absorb the power ripple. In contrast, from Fig. 11 (b), the proposed power decoupling method is controlled to actively fluctuate the buffer capacitor voltage  $v_{C_{buf}}$ . Consequently, the second-order harmonics in the DC input current is suppressed greatly.

Figure 12 shows the harmonic analysis of the input current. Note that the fundamental harmonic is based on the grid frequency component. The harmonic components of the input current up to 20th-order of the grid frequency are considered in this evaluation. It is confirmed from the analysis result, the ripple component (100 Hz) without the power decoupling method is 65.6%, which is normalized by the DC component of  $i_{dc}$ . In contrast, the proposed method reduces the second-order harmonics of the input current as shown in Fig. 11 (b) by 46.5%. Consequently, the experimental results verified the fundamental operation of the proposed power decoupling method. The input current ripple will be reduced more by improving the input current control performance and clarifying the optimized design to absorb the power ripple component.

## V. Conclusion

This paper proposed the DC to single-phase AC isolated converter with the boost-type topology of the power decoupling capability by the three-winding coupled inductor. The proposed system with the indirect matrix converter is expected to achieve down-sizing compared to the conventional rectifier-inverter system, because in the proposed system a bulky electrolytic capacitor for DC-link is not required. Moreover, the additional switching devices and magnetic component for the power decoupling operation do not required in the proposed method. In particular, leakage inductors of the coupled inductor are employed for the power decoupling circuit and the boost operation of the full bridge inverter. As a simulation result, the power ripple component as a secondary-order harmonics is reduced by 97.5% in comparison without the proposed power decoupling method. In addition, the experimental result verifies the proposed power decoupling method and the secondary-order harmonics caused by the power ripple reduced by 46.5%.

## References

- [1] K.Shiozaki, J.S.Lee, T.Nomura, B.Whitaker, A.Barkley, Z.Cole, B.Passmore, T.McNutt and A.B.Lostetter, "Design and Verification of High Frequency SiC On-board Vehicle Battery Charger for PHV/EV", SAE of Japan, pp. 25, (2014)
- [2] V.D.Doan, H.Fujimoto, T.Koseki, T.Yasuda, H.Kishi, and T.Fujita, "CSimultaneous Optimization of Speed Profile and Allocation of Wireless Power Transfer System for Autonomous Driving Electric Vehicles," IEEJ J.Industry Applications, vol. 7,no .2, pp. 189-201, (2018)

- [3] A. Tokumasu, K. Shirakawa, H. Taki, K. Wada : "AC/DC Converter Based on Instantaneous Power Balance Control for Reducing DC-Link Capacitance", IEEJ Journal of Industry Applications, Vol. 4, No. 6 pp.745-751 (2015)
- [4] K. H. Chao, P. T. Cheng: "Power Decoupling Methods for single-phase three-poles AC/DC converters", Proc. ECCE2009, pp. 3742-3747 (2009)
- [5] S. Yamaguchi, T. Shimizu: "Single-phase Power Conditioner with a Buck-boost-type Power Decoupling Circuit", IEEJ Journal of Industry Applications, Vol. 5, No. 3, pp.191-198 (2016)
- [6] Z. Qin, and others: "Benchmark of AC and DC Active Power Decoupling Circuits for Second-Order Harmonic Mitigation in Kilowatt-Scale Single-Phase Inverters", IEEE Journal of Emerging and Selected Topics in Power Electronics, Vol. 4, No. 1, pp.15-25 (2016)
- [7] T. Shimizu, K. Wada, N. Nakamura : "Flyback-Type Single-Phase Utility Interactive Inverter With Power Pulsation Decoupling on the DC Input for an AC Photovoltaic Module System", IEEE Trans. On Power Electronics, Vol. 21, No. 5, pp. 1264-1272 (2006)
- [8] C.T. Lee, Y.M. Chen, L.C. Chen, P.T.Cheng: "Efficiency Improvement of a DC/AC Converter with the Power Decoupling Capability", 2012 Twenty-Fourth Annu.IEEE Appl. Power Electron. Conf Expo., pp1462-1468, Feb.(2012)
- [9] Y. Tang, F. Blaabjerg, P. C. Loh, C. Jin, and P. Wang, "Decoupling of fluctuating power in single-phase systems through a symmetrical half-bridge circuit" IEEE Trans. Power Electron., vol. 30, no. 4, pp.1855–1865,(2015)
- [10] J. Itoh; T. Sakuraba; H. Watanabe; N. Takaoka: "DC to single-phase AC grid-tied inverter using buck type active power decoupling without additional magnetic component", 2017 IEEE ECCE, pp1765-1772 (2017)
- [11] N.Takaoka, H.Takahashi, J.Itoh: "Isolated Single-Phase Matrix Converter Using Center-Tapped Transformer for Power Decoupling Capability", IEEE Transactions on Industry Applications, Vol. 54, No. 2, pp. 1523-1531 (2018)
- [12] E.C. Nho, J.H.Jung, H.S.Kim: "Switching Loss Minimization of 3-phase Interleaved Bidirectional DC-DC Converter" The 2014 IPEC, pp2763-2764 (2014)
- [13] S.Kimura, K.Nanamori, T.Kawakami, J.Imaoka, and M.Yamamoto, "Allowable Power Analysis and Comparison of High Power Density DC-DC Converters with Integrated Magnetic Components,"IEEJ J. Industry Applications, vol. 6, no. 6, pp. 463-472, (2017)